Distributions of U^K_{37} and $U^K_{37'}$ in the surface waters and sediments of the Nordic Seas: Implications for paleoceanography

James Bendle

Environmental Research Centre, Department of Geography, University of Durham, Durham DH1 3LE, UK

Now at Organic Geochemistry Group for the Study of the Ocean and the Atmosphere, Institute of Low Temperature Science, Hokkaido University, N19, W8, Kita-ku, Sapporo, 060–0819, Japan (bendle@pop.lowtem.hokudai.ac.jp)

Antoni Rosell-Melé

ICREA and Institut de Ciència i Tecnologia Ambientals, Universitat Autònona de Barcelona, 08193 Bellaterra, Catalonia, Spain (antoni.rosell@icrea.es)

Also at Department of Geography, University of Durham, Durham DH1 3LE, UK

[1] In this paper we revise the application of the $U^K_{37'}$ and U^K_{37} indices as sea surface temperature (SST) proxies in the Nordic Seas. In the summer of 1999 and 2000 we obtained samples of filtered particulate organic matter (POM) from surface waters ($\sim$6 m depth) of the Nordic Seas. A number of samples were collected from polar waters with up to 80% of sea ice cover. Alkenones were detected in all of the major water masses of the Nordic seas, across a spectrum of SST values from -0.5 to 13°C and SSS values from 29.6 to 35.6 (psu). Concentrations of alkenones were similar in magnitude to those reported previously for the North Atlantic and the Southern Ocean. Values of $U^K_{37'}$ from the new Nordic Seas POM data show no correlation with SST below 8°C. In contrast, below this temperature a linear correlation exists between U^K_{37} and regional SST, supporting previous suggestions that, overall, U^K_{37} may be a more appropriate SST index for the region. It must be noted however that U^K_{37} is calculated using the tetraunsaturated alkenone, and the dominant control on this compound is not yet fully understood. The new data highlight major differences between distributions of U^K_{37} and $U^K_{37'}$ in the water column POM and surficial sediments of the Nordic Seas. We also examine the geographical dependence of the $U^K_{37'}$ versus SST relationship in the region's surficial sediments. Some areas are associated with unreliable SST estimates, whereas in others the $U^K_{37'}$ versus SST relationship falls within the range of a global core top calibration. It is suggested that the breakdown of the $U^K_{37'}$-SST relationship in some regions is due to ecological and sedimentological factors. The latter relates to the extension of the habitats of alkenone producers in polar waters. The former to the resuspension of sediments and laterally transported alkenone inputs. This suggests that accurate alkenone derived SST estimates in the Nordic seas are geographically constrained.

1. Introduction

[2] Since it was first demonstrated that alkenone abundance ratios in sediments changed in a systematic way with inferred sea surface or measured water growth temperature of the alkenone producing organisms [*Brassell et al.*, 1986a, 1986b; *Conte and Eglinton*, 1993; *Conte et al.*, 1992; *Marlowe*, 1984; *Prahl et al.*, 1988; *Prahl and Wakeham*, 1987], a great deal of research has been conducted with the aim of confirming and calibrating this relationship. The U$_{37}^{K}$ index was initially defined as [*Brassell et al.*, 1986b]

$$U_{37}^{K} = \frac{C_{37:2} - C_{37:4}}{C_{37:2} + C_{37:3} + C_{37:4}},$$

but because the C$_{37:4}$ alkenone is often absent or not detectable in middle to low latitudes, the ratio was simplified to [*Prahl and Wakeham*, 1987]

$$U_{37'}^{K} = \frac{C_{37:2}}{C_{37:2} + C_{37:3}}.$$

The dependence of the relative abundance of the C$_{37:2}$ and C$_{37:3}$ alkenones with water temperature has been confirmed by culture, surficial sediment and water column particulate organic matter (POM) studies [e.g., *Brassell*, 1993; *Muller et al.*, 1998; *Prahl et al.*, 1988, 2000; *Prahl and Wakeham*, 1987; *Rosell-Melé et al.*, 1995a; *Sikes and Volkman*, 1993; *Sikes et al.*, 1997; *Sonzogni et al.*, 1997; *Ternois et al.*, 1997] (also see review by *Herbert* [2001]). Therefore U$_{37'}^{K}$ when measured in most modern sediments throughout the world ocean can be converted into realistic, seemingly reliable estimates of mean annual temperature at the sea surface (SST). Moreover, it appears that values of U$_{37'}^{K}$, once set biogeochemically by the algae, are not significantly altered by degradation in sedimentary processes [e.g., *Conte et al.*, 1992; *Freeman and Wakeham*, 1991; *Madureira et al.*, 1995; *Prahl and Muehlhausen*, 1989; *Teece et al.*, 1998] (also see review by *Grimalt et al.* [2000]).

[3] However, despite such positive results, the application of alkenone indices are not devoid of uncertainties. The initial U$_{37'}^{K}$-SST calibration derived from a culture of *E. huxleyi* (N.E. Pacific strain) by *Prahl and Wakeham* [1987] shows a clear linear relationship between U$_{37'}^{K}$ and temperature in the range of 8–25°C. Interestingly, this linear regression equation is statistically the same as a regression between U$_{37'}^{K}$ measured in global (60°N–60°S) sediment core tops and ocean-atlas mean annual SSTs [*Muller et al.*, 1998]. However,

a number of culture studies on *E. huxleyi* and *G. oceanica* strains from various oceanographic locations have produced different slopes for the relationship of U$_{37'}^{K}$-SST (see *Herbert* [2001] for review). Also, there is a systematic difference in the slope of the U$_{37'}^{K}$-SST relationship, derived from global water column POM samples [*Conte and Eglinton*, 1993; *Harada et al.*, 2003; *Sicre et al.*, 2002; *Sikes and Sicre*, 2002; *Sikes and Volkman*, 1993; *Ternois et al.*, 1997, 1998] and the data from the culture by *Prahl and Wakeham* [1987] and from core tops by *Muller et al.* [1998], whereby the water column POM data generally give warmer-than-predicted growth temperatures at a given U$_{37'}^{K}$, particularly in the range ∼5–15°C. Furthermore, a number of studies highlight a degree of nonlinearity in the relationship of alkenones to SST at high (>25°C) and low (<8°C) temperature extremes [*Conte et al.*, 2001; *Pelejero and Calvo*, 2003; *Rosell-Melé*, 1998; *Sikes and Volkman*, 1993; *Sonzogni et al.*, 1997].

[4] Therefore it is apparent that in certain contexts or regions absolute temperatures derived from the "recommended" *Prahl and Wakeham* [1987] or *Muller et al.* [1998] equations are unrealistic. It has been suggested by *Rosell-Melé et al.* [1995c] that this may apply to the Nordic Seas region, where, on the basis of an extensive core top data set, considerable scatter is seen in the U$_{37'}^{K}$-SST relationship. In this region it is has been suggested that a calibration based on the original U$_{37}^{K}$ index, which incorporates the C$_{37:4}$ compound, gives more accurate results down to 6°C [*Rosell-Melé*, 1998]. This contrasts with the cold waters of the southern ocean, where U$_{37'}^{K}$ is well correlated to SST down to ∼3°C, or in the South Atlantic where the correlation reaches 0°C [*Sikes et al.*, 1997]. In the Nordic Seas, below 6°C, neither the U$_{37'}^{K}$ nor U$_{37}^{K}$ index, measured in surface sediments, is correlated to SST. This is frustrating for paleoceanographic investigations, as the cold water regions of the Nordic Seas play a key role in the production of deep water masses, and in the wider global meridonal overturning circulation (MOC).

[5] The Nordic Seas surface current system is characterized by the interaction of relatively warm (6–15°C) and saline (>35 psu) Atlantic source waters and cold (<5°C), less saline (<34.4 psu) polar source waters across strong east to west hydrographic gradients. The Atlantic inflow reaches the Nordic seas via the Greenland-Scotland ridge and has several branches (Figure 1). The advection of north Atlantic water (even as far as the Kara sea) has a profound influence on the
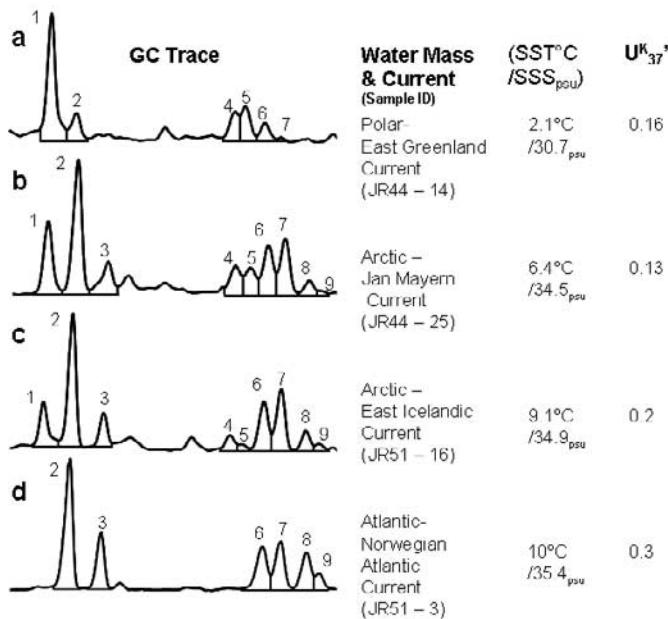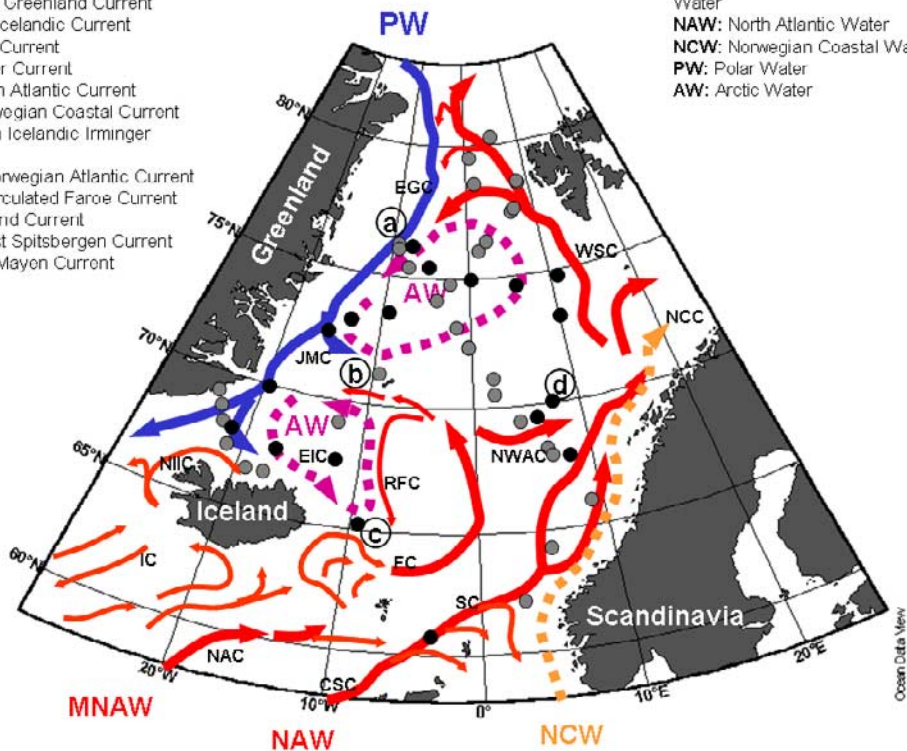
Figure 1. Map showing the sampling locations during two ARCICE cruises on the RRS *James Clark Ross* from mid-July to September 1999 (JR44, gray dots) and 2000 (JR51, black dots). Main features of the surface to near-surface circulation the Nordic Seas are illustrated. Sources: *Hansen and Østerhus* [2000]; *Johanessen* [1986]; *Swift* [1986]. Representative GC-FID traces of alkenone patterns from different water masses are also illustrated. Alkenone peak assignment: (1) $C_{37:4}$ Me; (2) $C_{37:3}$ Me; (3) $C_{37:2}$ Me; (4) $C_{38:4}$ Et; (5) $C_{38:4}$ Me; (6) $C_{38:3}$ Et; (7) $C_{38:3}$ Me; (8) $C_{38:2}$ Et; (9) $C_{38:2}$ Me.

Northern seas and climate of Western Europe, releasing a large amount of sensible heat ($\sim 5 \times 10^{21}$ cal/yr) to the atmosphere [*Broecker and Denton*, 1989; *Dickey et al.*, 1994]. Polar waters enter the eastern upper layers of the region from the Arctic Ocean [*Swift*, 1986]. The East Greenland Current (EGC) carries polar water southward and out through the Denmark Strait (Figure 1), while two branches transport small amounts eastward into the interior basins; the Jan Mayen Current (JMC), to the north of the Jan Mayen Fracture Zone, and the East Icelandic Current (EIC), which flows southeast along the continental slope northeast of Iceland (Figure 1) [*Swift*, 1986]. Between the regions dominated by the polar and Atlantic source waters, lies a region where the two source waters mix in two anticlockwise gyres. These regions are characterized by upper layer waters that are (in winter) relatively cold (0 to 4°C) and saline (34.6 to 34.9 psu). In this Arctic Province (or Arctic Waters AW) the surface waters are denser than either of the surface source-water masses ($\sigma_t =$ 27.5 to 28+) [*Swift*, 1986]. This dense AW contributes greatly to the vertical instability of the region; so that winter cooling and wind mixing cause strong deep convection contributing to the formation of deep water masses [e.g., *Dickson and Brown*, 1994].

[6] Further investigation of alkenone distributions in the Nordic seas surface waters is necessary, as previous North Atlantic water column studies have reported no [*Conte and Eglinton*, 1993; *Thomsen et al.*, 1998] or very few [*Sicre et al.*, 2002] results from the Arctic and Polar water masses. Widespread water column POM data are needed to complement previous studies of alkenone distributions in surface sediments [*Rosell-Melé*, 1998; *Rosell-Melé et al.*, 1995c]. In this study we report alkenone distributions measured in sea surface ($\sim$6 m depth) POM obtained from across the spectrum of property gradients (i.e., covering all the characteristic water masses) of the Nordic seas, during two cruises of the RRS *James Clark Ross* (*JCR*) in 1999 and 2000. In this study we obtained samples from the ships uncontaminated seawater supply at a fixed depth of 6m. This enabled us to filter large volumes of water from the mixed layer for a relatively large number of samples from a wide geographic area without stopping the ship for sampling. This sampling strategy was designed to gain an insight into the spatial variability of alkenone data. The advantage of studying water column POM is that alkenone distributions can be directly compared to ocean parameters in situ;

therefore a precise reflection of the local correlation between alkenone unsaturation and growth temperature may be derived. The approach provides a brief temporal "snap shot" measurement of environmental conditions, rather than an integrated seasonal signal, as can be inferred from sediment traps or bottom sediments data. Hence the importance of repeating the sampling in subsequent years, as we did, to appraise to some extent the interannual variability of the data. This is also useful to appraise another potential limitation of our study, which is the potential temporal offsets that might have existed between the time of alkenone synthesis and our sampling. However, we sampled the Nordic seas during the midsummer when grazing by zooplankton has reached a peak and, although primary productivity is high, the standing stock of the phytoplankton is greatly reduced (compared to the spring "bloom"). [e.g., *Lalli and Parsons*, 1997; *Longhurst*, 1998]. During this period the chances of obtaining samples consisting of a significant proportion of old/senescent material was, in principle, minimal.

[7] The objective of this paper is to clarify and delimit the application of the $U^K_{37'}$ and U^K_{37} alkenone proxies for paleoceanographic studies in the subpolar to polar regions of the Nordic Seas. To this end we compare alkenone distribution data from sea surface POM samples with previously reported sedimentary data from the Nordic Seas. Secondarily we place the Nordic Seas sea surface POM data in a global context by comparison with a global data set. Detailed reports of other alkenone data obtained ($\%C_{37:4}$) will be published elsewhere (J. Bendle et al., Interannual variability and paleoceanographic implications of unusual distributions of alkenones in the surface waters of the Nordic Seas, submitted to *Paleoceanography*, 2004) (hereinafter referred to as Bendle et al., submitted manuscript, 2004).

2. Materials and Methods

2.1. Sample Retrieval

[8] Seawater POM was obtained onboard the RRS *James Clark Ross* during the NERC Arctic Ice and Environmental Variability (ARCICE) summer cruises "JR44" in 1999 (25/7/99–28/8/99) and "JR51" in 2000 (28/7/00–29/8/00). Sample details are given in Tables 1 and 2; sample locations are indicated in Figure 1. The POM was filtered from seawater collected in the laboratory from the uncontaminated supply which was continuously

Table 1. JR44 Filter Sample Information[a]

Sample	Coordinates Latitude, N	Longitude, E	Date (1999)	Vol. Filtered, L	SST, °C	SSS, psu	ΣC_{37}, ng/L	ΣLCK, ng/L	GC-CI-MS C_{37} Isomer Response, mV*min $C_{37:4}$	$C_{37:3}$	$C_{37:2}$	$U_{37'}^K$	U_{37}^K
1	62°21.36′	3°20.60′	24/07	140	13.2	34.73	32.0	54.5	ND	206929	153591	0.43	0.43
2	64°17.57′	5°40.33′	25/07	140	12.7	34.72	25.4	43.8	ND	205390000	112720000	0.35	0.35
3	65°98.46′	8°88.64′	26/07	140	11.9	34.21	8.7	16.4	5975508	91459560	35478504	0.28	0.22
4	67°90.32′	6°74.48′	27/07	140	11	35.12	5.2	7.7	ND	79296864	45364996	0.36	0.36
5	68°20.02′	6°37.71′	27/07	140	10.9	35.12	1.7	2.6	ND	40803472	20873120	0.34	0.34
6	69°57.68′	4°55.16′	28/07	140	9.6	35.10	35.4	59.9	2878132	66447996	19934856	0.23	0.19
7	70°79.43′	2°71.61′	29/07	140	9.3	35.06	21.8	36.5	748907	65685644	22069924	0.25	0.24
8	71°13.66′	2°15.05′	29/07	140	9.3	35.17	ND	ND	1269309	40100300	9470588	0.19	0.16
9	72°55.85′	−0°39.61′	30/07	130	6.6	34.92	8.6	13.4	236993	25049286	5860770	0.19	0.18
10	73°07.34′	−1°47.05′	30/07	140	5.4	34.72	ND	ND	-	-	-	-	-
11	74°13.35′	−3°82.23′	31/07	140	5.1	34.71	ND	ND	-	-	-	-	-
12	75°56.82′	−7°75.95′	01/08	140	5	34.61	ND	ND	-	-	-	-	-
13	76°03.46′	−9°24.27′	02/08	140	0.3	30.71[b]	ND	ND	4248410	1400932	186463	0.12	−0.70
14	76°37.29′	−10°45.94′	02/08	140	2.1	30.69[b]	4.7	6.9	21389678	5363385	1058775	0.16	−0.73
15	80°41.69′	5°54.62′	10/08	140	4.9	34.41[b]	4.6	7.9	2644676	18029870	4616426	0.20	0.08
16	79°86.56′	1°02.52′	13/08	140	2.1	34.28[b]	1.6	3.0	7610967	9445704	1929831	0.17	−0.30
17	78°88.35′	1°77.0.3′	14/08	140	1.8	33.03[b]	3.3	5.4	18877274	8972016	1634382	0.15	−0.58
18	78°83.32′	8°72.3.5′	15/08	140	7.1	34.81[b]	1.4	2.5	1393344	7569482	2178028	0.22	0.07
19	78°71.48′	9°05.20′	15/08	140	7	34.81[b]	1.1	1.9	391375	3699818	1313646	0.26	0.17
20	77°51.98′	7°28.52′	16/08	140	6.7	35.04[b]	ND	ND	-	-	-	-	-
21	77°39.36′	6°68.68′	16/08	140	6.7	35.03[b]	ND	ND	-	-	-	-	-
22	76°34.34′	2°66.92′	17/08	140	6	34.90[b]	ND	ND	-	-	-	-	-
23	76°00.41′	1°51.32′	17/08	140	5.7	34.88[b]	ND	ND	-	-	-	-	-
24	74°76.20′	−2°16.21′	18/08	110	5.3	34.74[b]	ND	ND	-	-	-	-	-
25	71°25.01′	−9°59.78′	20/08	140	6.4	34.71[b]	7.8	13.2	72028552	159000000	24361404	0.13	−0.19
26	69°22.85′	12°66.74′	21/08	140	6.8	34.66[b]	1.8	3.2	896431	5648757	1328236	0.19	0.05
27	66°86.66′	17°39.28′	22/08	140	8.5	34.41[b]	7.2	12.4	94041	1723457	568590	0.25	0.20
28	67°48.49′	21°51.18′	23/08	140	6.1	34.06[b]	20.3	33.3	765802	9333642	2038687	0.18	0.10
29	68°71.13′	23°01.14′	24/08	140	4.2	29.65[b]	ND	ND	-	-	-	-	-
30	69°22.79′	23°70.43′	24/08	140	2.5	30.93[b]	ND	ND	-	-	-	-	-
31	68°13.55′	22°28.25′	25/08	140	4.4	33.07[b]	ND	ND	-	-	-	-	-
32	66°69.5′	18°36.52′	26/08	140	7.2	33.58[b]	18.0	30.4	559376	8531252	2315096	0.21	0.15

[a] Collection and analytical data SST, SSS were measured using the ships' data logging systems except where indicated. ΣC_{37} and ΣLCK are the total abundance of the C_{37} alkenones only and the C_{37} + C_{38} alkenones, respectively, as measured by GC-FID. ND stands for "not detected." A hyphen indicates that the parameter was not measured or calculated.

[b] Derived from CTD rather than ships' thermosalinograph. CTD profiles were obtained from the same oceanographic station as the POM collection; we use the SST and SSS measurements made at ~6 m depth.

pumped to the ship laboratories from a supply tube beneath the hull. The depth of the tube inlet beneath the sea surface was approximately at 6m. A seawater sample (volume 60–153 L) was collected into carboys and filtrated through a manifold of funnel/flask apparatus holding Whatman 70 mm GF/F glass fiber filters (precleaned by firing at 450°C) (during JR44 the particulate suspension was concentrated prior to filtering using a Millipore Pellicon tangential flow system). The POM laden filters for a station were placed into a clean 50 ml Teflon capped (aluminum foil lined) glass bottles using clean forceps. A 100 ml mixture of dicloromethane (DCM)/methanol (MeOH) (3:1) was added and the sample was then sealed and stored in a freezer until analysis.

[9] In situ environmental data (SST, SSS, fluorescence) were logged during the cruises using the ships oceanlogger system. SST was measured by a probe mounted near the hull close to the uncontaminated water inlet. Salinity and fluorescence were measured, from the uncontaminated supply, by a SeaBird SBE45 thermosalinograph and Turners Instruments fluorometer located in one of the ship's laboratory. The ocean logger data (measurements made every 1 s) were used to derive sea surface property maps and to calculate mean values of SST and SSS for the period (~20 min) when each POM sample was collected (i.e., the SST and SSS values in Tables 1 and 2). During cruise JR44, the salinity from 2/8/1999 onward (filter sample no.13) was taken from the top of the CTD profile

Table 2. JR51 Filter Sample Information[a]

Sample	Coordinates Latitude, N	Longitude, E	Date (1999)	Vol. Filtered, L	SST, °C	SSS, psu	ΣC_{37}, ng/L	ΣLCK, ng/L	GC-CI-MS C_{37} Isomer Response, mV*min $C_{37:4}$	$C_{37:3}$	$C_{37:2}$	$U_{37'}^K$	U_{37}^K
1	67°78.83′	7°75.10′	28/7	60	10.6	34.75	11.1	19.1	138944	28403218	11128898	0.28	0.28
2	69°39.56′	5°50.00′	28/7	100	10.1	35.32	3.4	5.9	ND	5571485	3113115	0.36	0.36
3	69°94.05′	7°09.67′	5/8	96	10.0	35.42	44.2	82.8	ND	42972372	18199352	0.30	0.30
4	73°16.66′	9°66.82′	6/8	153	8.0	35.45	ND	ND	-	-	-	-	-
5	74°66.67′	10°49.99′	6/8	85	7.5	35.40	1.9	3.2	1075359	20662586	9024364	0.30	0.26
6	74°49.86′	5°36.53′	8/8	78	7.3	35.39	ND	ND	ND	1866330	1053238	0.36	0.36
7	74°81.77′	−0°06.03′	9/8	153	5.9	35.15	ND	ND	-	-	-	-	-
8	76°02.65′	−7°64.46′	10/8	120.5	−0.6	30.72	1.9	2.9	17006148	9001958	2214277	0.20	−0.52
9	75°29.56′	−5°18.79′	11/8	148.5	5.6	34.70	ND	ND	-	-	-	-	-
10	73°44.07′	−9°43.56′	14/8	119	3.4	31.96	ND	ND	-	-	-	-	-
11	73°02.72′	−13°43.83′	17/8	151	3.5	31.20	ND	ND	-	-	-	-	-
12	72°42.87′	−15°52.58′	24/8	127.5	1.8	30.87	3.8	5.4	276985	218103	46982	0.18	−0.42
13	69°81.30′	−19°39.40′	25/8	149.5	0.8	30.12	ND	ND	5043562	3519187	1136476	0.24	−0.40
14	67°87.74′	−21°32.05′	26/8	100.5	7.0	34.24	57.0	109.5	7565562	44364412	7282673	0.14	0.00
15	67°55.15′	−17°12.47′	26/8	110	7.6	34.71	22.8	39.4	6097162	37779684	9193764	0.20	0.06
16	67°52.07′	−12°08.94′	27/8	104.5	9.1	34.87	7.1	13.2	4041261	22381554	5469366	0.20	0.04
17	65°09.01′	−9°40.69′	28/8	142	8.8	34.98	ND	ND	2974084	40025916	6498169	0.14	0.07
18	60°66.16′	−3°59.03′	29/8	79	12.9	35.60	4.4	6.9	ND	19853816	12809840	0.39	0.39

[a] Collection and analytical data SST, SSS were measured using the ships data logging systems except where indicated. ΣC_{37} and ΣLCK are the total abundance of the C_{37} alkenones only and the $C_{37} + C_{38}$ alkenones, respectively, as measured by GC-FID. ND stands for "not detected." A hyphen indicates that the parameter was not measured or calculated.

obtained at the same station, due to a malfunction of the ocean logger conductivity sensors [*Bacon and Yelland*, 1999].

[10] The majority of surface sediment data used in this study was obtained from a series of boxcores recovered by successive cruises of the German vessel the *Meteor* between 1987 and 1989 (the top 1 cm was subsampled for surface sediment values). Alkenone data from these samples has been used in several previous papers [*Rosell-Melé*, 1998; *Rosell-Melé et al.*, 1993, 1995b]. We use the SST and SSS values that were assigned to the samples for a previous paper [*Rosell-Melé*, 1998], i.e., World Ocean Atlas mean summer values (July, August, September) at 0 m depth [from *Levitus and Boyer*, 1994]. Several additional core top samples for the Icelandic shelf region of the Nordic Seas were taken from gravity cores collected during ARCICE cruises JR44 and JR51, SST and SSS values for these samples were assigned using summer values at 0 m depth from the latest version of the World Ocean Atlas [*Conkright et al.*, 1998].

2.2. Analytical Methods

[11] The glass fiber filters containing the particulate material were extracted by ultrasonication (×3) with 20 ml of DCM/MeOH (3:1), after addition of an internal standard. The combined extracts were hydrolyzed in sealed test tubes with a 3 ml solution of potassium hydroxide (KOH)/MeOH 8% for 36 hrs. The neutral fraction was recovered with 3 ml of hexane (×3) and the combined extract was washed with water (previously distilled and solvent extracted), in a test tube to remove residual KOH traces. The extract was redissolved, dried with sodium sulfate and stored sealed, at −20°C, until analysis.

[12] Analytical methods for old sediment samples are described by *Rosell-Melé* [1998]; new samples, obtained during JR51, were freeze-dried and ground and an internal standard was added and extracted with DCM/MeOH at 70°C for 5 min using a MARS 5 microwave extractor [*Kornilova and Rosell-Melé*, 2003]. The solvent extract was concentrated to dryness by centrifugal evaporator or with nitrogen blow-down, redissolved in DCM and dried with sodium sulfate.

[13] Sediment extracts were fractionated by High Performance Liquid Chromatography (HPLC). This was performed using a system consisting of a Thermo Hypersil column (50 × 4.6 mm) packed with Lichospher Si100 5 μm silica, and a Thermo Hypersil guard column. Fractions were collected using a Foxy Jr automatic collector. The solvent program was adapted from *Schulz et al.* [2000]. Four fractions were collected in test tubes

by eluting at 1 ml min^{-1} with: hexane (1.75 ml, aliphatic and cyclic alkanes), hexane/DCM (17:3; 3.5 ml, aliphatic ketones), DCM (2.25 ml, cyclic ketones), acetone (2.25 ml, sterols, alcohols and polars). Fractions 1 and 2 were combined, dried under nitrogen and derivatized using bis-trimethyl-silyl-trifluoroacetamide (BSTFA) prior to gas chromatographic analysis.

[14] Quantification of the absolute abundance of alkenones was performed using a Fisons 8000 Series gas chromatograph fitted with a flame ionization detector (GC-FID) and a split/splitless injector. Baseline separation of the alkenones was obtained using a SGE BP-1 fused silica column (60 m × 0.25 mm i.d., coated with 0.25 μm film thickness), and an oven temperature program as follows: 60°C for 1 min, 60°C to 200°C at 20°C min^{-1}, 200°C to 305°C at 6°C min^{-1}, held at 305°C for 35 min, 305°C to 320°C at 15°C min^{-1} and held at 320°C for 2 min. Hydrogen was used as a carrier gas.

[15] Analysis of the relative abundances of the target compounds (within-class-distributions) was performed using a Varian 3400 gas chromatograph directly coupled to a Finnigan MAT TSQ 700 triple stage quadrupole mass spectrometer (GC-CI-MS), using ammonia chemical ionization [*Rosell-Melé et al.*, 1995a]. The GC was fitted with a splitless injector operated in "high performance" nonvaporizing mode, held at 80°C during injection then rapidly heated from 80–300°C at 200°C min^{-1}. Separation of the analytes was achieved using a 50 m, 0.32 mm i.d. fused silica column, with 0.12 μm CPSIL5-CB film thickness (Chrompack). The oven temperature program was: 200–300°C at 6°C min^{-1} with no initial hold time and a final isothermal period of 10 min. Hydrogen was employed as a carrier gas with a head pressure of 8 psi. Operating conditions for the mass spectrometer were optimized for sensitivity with respect to the C_{37} methyl alkenones. Chemical ionization was achieved using high purity ammonia (BOC micrographic grade). Specific ions, corresponding to the $[M + NH_4]^+$ species of the analytes were monitored.

[16] Procedural and analytical reproducibility was determined for the analyses with an homogeneous "sediment standard" (analyzed once for every 10 samples to be validated). The overall average reproducibility for the absolute quantification of alkenones by GC-FID had a coefficient of variation (CV) of 5.92% (at 2σ). The overall average reproducibility for $U^K_{37'}$ and U^K_{37} by GC-CI-MS at 2σ was 0.017 ($U^K_{37'}$ units) and 0.02 (U^K_{37} units), respectively.

3. Results and Discussion

3.1. In Situ Oceanography

[17] The complex systems of warm and cold currents in the Nordic Seas (Figure 1) are arbitrarily delimited by a number of ocean fronts, which reflect strong quasi-permanent boundaries in the temperature and salinity fields and which are strongly associated with the bottom topography [*Johanessen*, 1986]. During the 1999 and 2000 ARCICE cruises the positions of the Polar Front (PF), Arctic Front (AF) and Norwegian Coastal Front (NCF) were estimated by comparison of the monitored sea surface property data and the typical Nordic Seas hydrographic provinces described in the literature (Figures 2a and 2b) [*Hansen and Østerhus*, 2000; *Johanessen*, 1986; *Swift*, 1986]. Additionally, depth profile data collected during both cruises by CTD (conductivity, temperature depth probe) and XBT (expendable bathythermograph probe) were also consulted [*Bendle*, 2003]. The SSS isoline at 34.4 psu was used to estimate the position of the PF, the 35 psu isoline was used to estimate the position of the AF (in the northwest) and the NCF (in the southeast). The position and extent of sea-ice off the east coast of Greenland was also estimated from SeaWiFS images of chlorophyll *a* (Figures 3a and 3b). The assignation of certain opaque areas in the SeaWiFS chlorophyll images as sea-ice (rather than cloud) was confirmed by reference to SeaWiFS true color images (not shown) (http://seawifs.gsfc.nasa.gov/SEA-WIFS.html).

[18] Comparison of Figures 1 and 2 reveals that filter samples were successfully obtained from all the major water masses in both 1999 and 2000 but that there was considerable variation in the position of the fronts between the two cruises. In 1999, the PF follows the continental shelf (Figure 2a), relatively closely especially south of ∼74°N. Also, the dense sea-ice does not extend south beyond a position level with the Hold with Hope Peninsula (Greenland) at 74°N (Figure 3a). In 1999 the AF follows, relatively closely, the line of the Mohns ridge, a position often ascribed as typical for the AF in reviews of Nordic Seas oceanography [e.g., *Johanessen*, 1986] (see Figure 2a). This results in a fairly large expanse of AW occupying the Greenland Sea between the Polar waters of the EGC in the west and the Atlantic signature waters in the
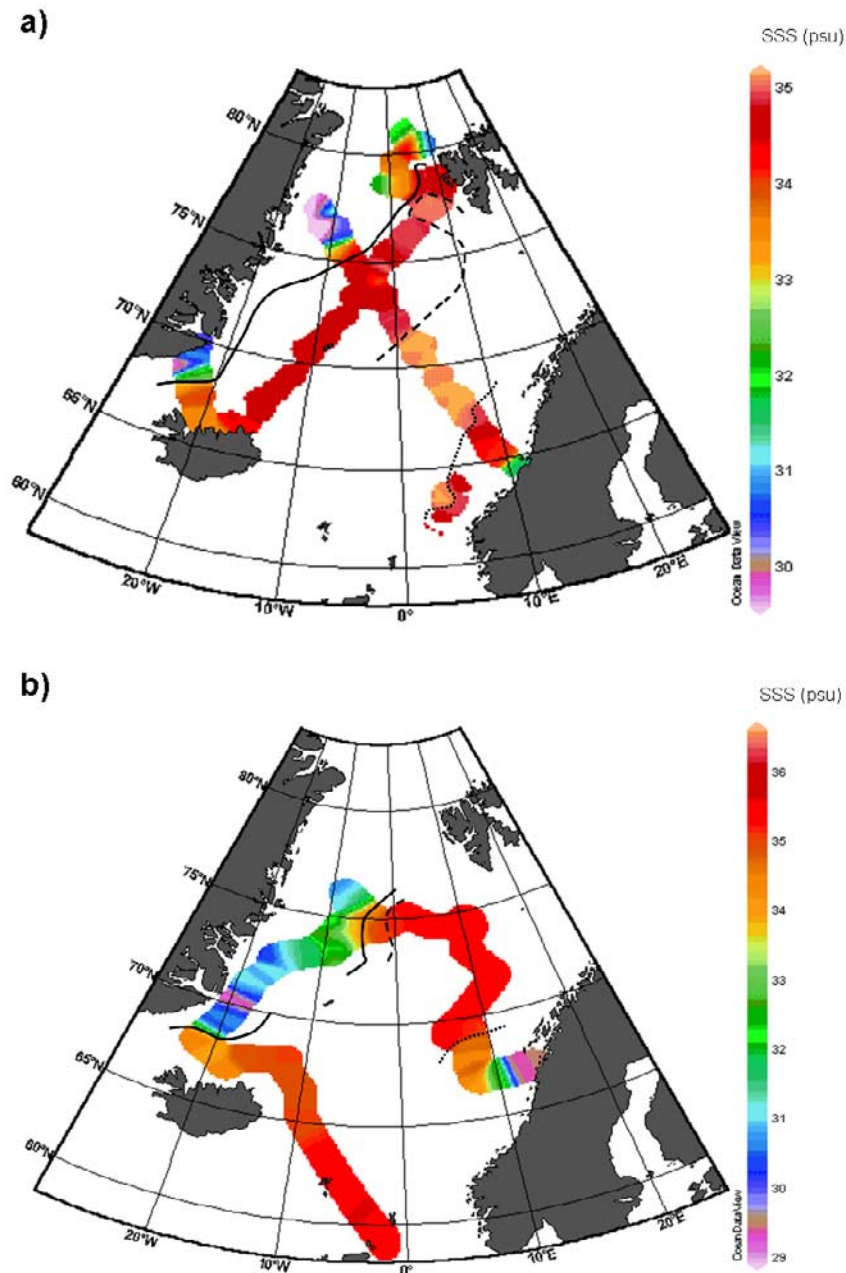
Figure 2. In situ measurements of sea surface salinity and estimated position of oceanographic fronts during cruises (a) JR44 and (b) JR51. PF, Polar Front; AF, Arctic Front; NCF, Norwegian Coastal Front.

Norwegian Sea to the east. In the north-eastern Nordic Seas, the West Spitsbergen Current (WSC) was observed to carry Atlantic signature waters fairly far north to ~78°N where there appears to be a sharp gradient to Polar type waters at ~80°N. In 1999, the NCF followed, the Norwegian continental shelf (see Figure 2a).

[19] The cruise track in 2000 did not extend as far to the northeast, therefore interannual comparisons

for this region are not possible. However, in the central, southern and western Nordic Seas, there was a degree of overlap and therefore comparisons can be made. In August 2000 there appeared to be some significant differences in the physical oceanography of the Nordic Seas compared to 1999. In the southwest Nordic Seas, in August 2000, the PF extended much further from the continental shelf (Figure 2b). The sea-ice also extends further south to a position level with
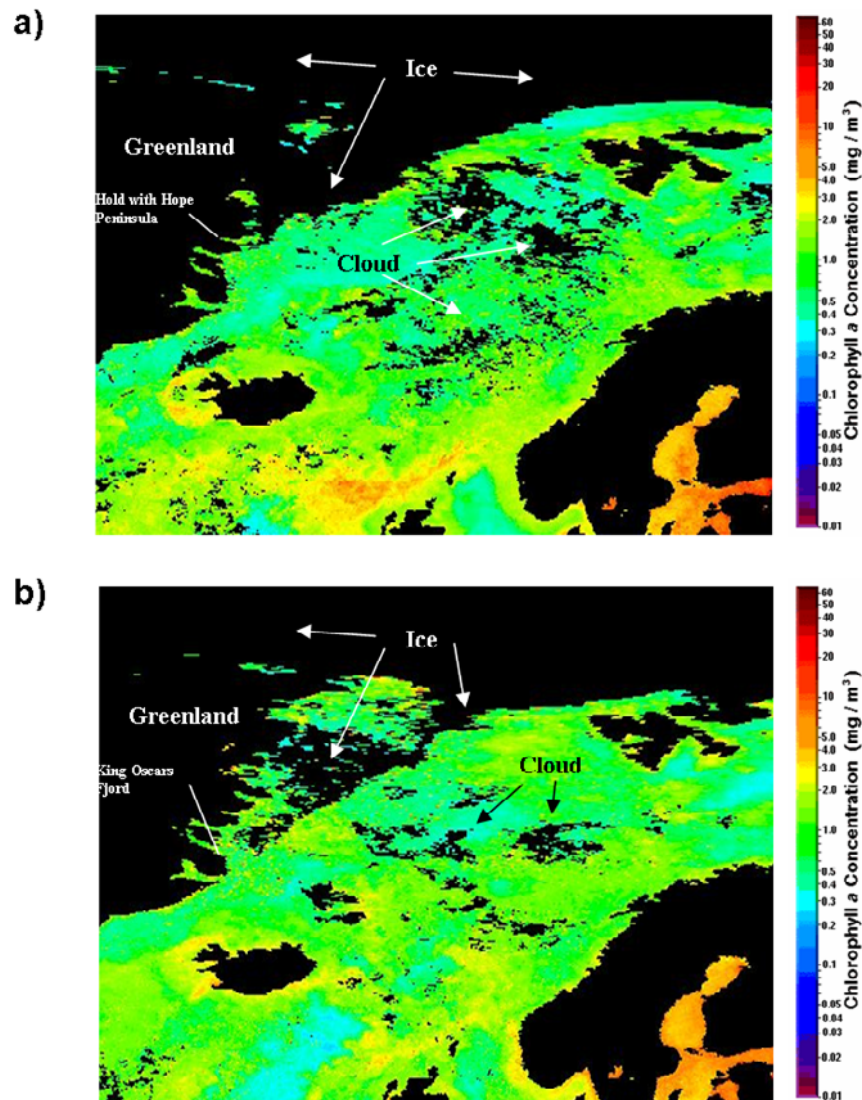
Figure 3. Chlorophyll *a* measurements for cruises (a) JR44 and (b) JR51. Color gridding shows remotely sensed CZCS chlorophyll *a* concentrations for August (a) 1999 and (b) 2000. Dark areas are ice, land or cloud (provided by the SeaWiFS Project, NASA/Goddard Space Flight Center and ORBIMAGE).

the King Oscar's Fjord (Greenland) at 72°N (Figure 3b). However, there appeared to be a larger opening of the ice-pack further North, compared to August 1999, with a large polynya visible to the northeast of Greenland (Figure 3b). In 1999 the AF followed the line of the Mohns ridge (see Figure 2a), with a fairly large expanse of AW occupying the Greenland Sea. This contrasts with the situation in 2000 where the PF and AF are, geographically, much closer in the central Nordic seas, due to the PF occupying a position further east and Atlantic signature waters pushing much farther west into the Greenland Sea. In 2000 the NCF pushed father west from the

Norwegian continental shelf compared to 1999 (Figures 2a and 2b).

3.2. Alkenone Absolute Abundance

[20] Alkenones were detected in all of the major water masses of the Nordic seas, across a spectrum of SST values from −0.5 to 13°C and SSS values from 29.6 to 35.6 (psu). The spatial and water mass distribution of alkenone abundances are illustrated in Figure 4. Concentrations of $C_{37} + C_{38}$ alkenones (ΣLCK) and C_{37} alkenones only (ΣC_{37}), as measured by GC-FID, ranged from 1.8 to 109.5 ng/L and 1.1 to 57.0 ng/L of filtered seawater, respec-
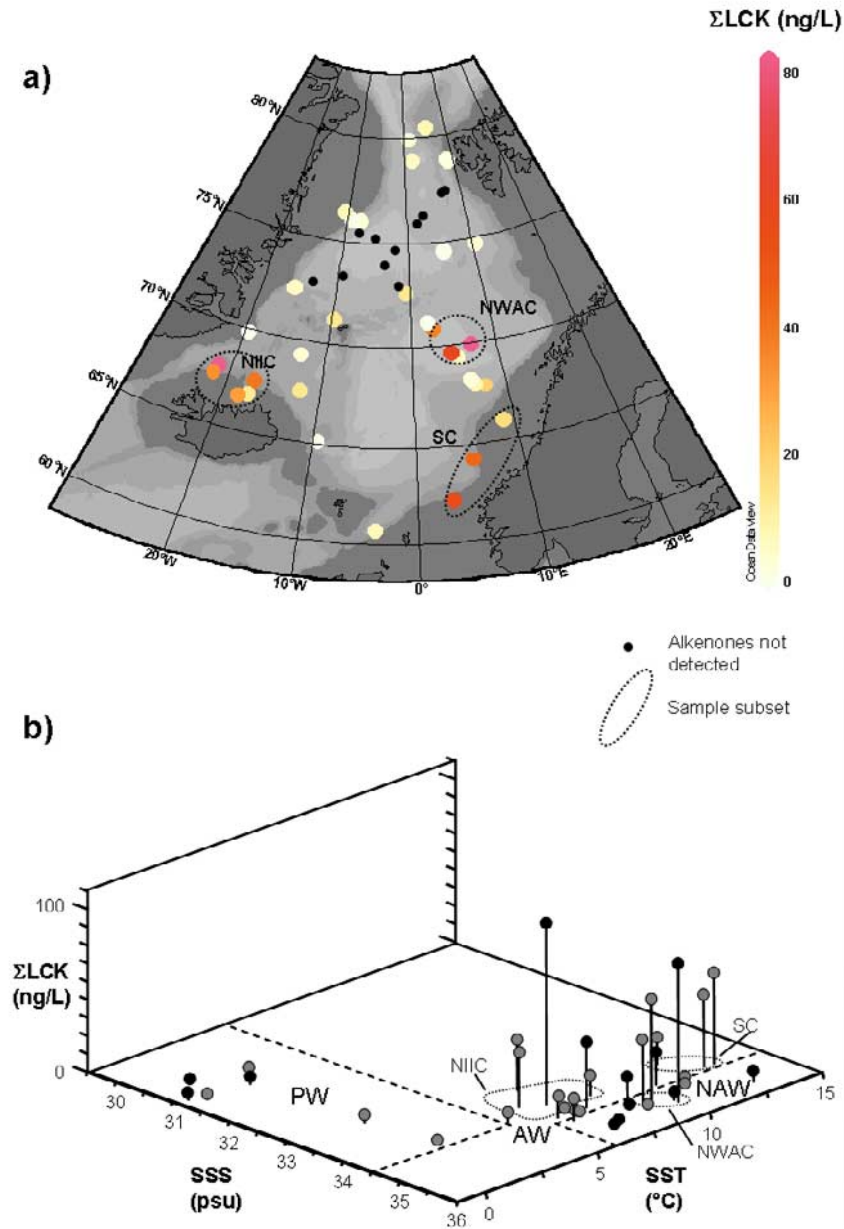
Figure 4. (a) Geographic distribution of ΣLCK (ng/L) in the surface waters of the Nordic Seas. Sample subsets obtained from the North Icelandic Irminger Currents (NIIC), Shetland Current (SC) and the Norwegian Atlantic Current (NWAW) are highlighted (dotted lines). (b) The same data from a 3-D perspective. Gray circle symbols are samples from JR44; black circle symbols are samples from cruise JR51.

tively. These concentrations are of a similar order of magnitude to those reported previously for the North Atlantic (ΣC_{37} ng/L mean = 48.3, s.d. = 23 [*Conte and Eglinton*, 1993]), the Nordic Seas (ΣC_{37} ng/L mean = 36.1, range = 1 to 156 [*Sikes and Sicre*, 2002]), and the Southern Ocean (ΣC_{37} ng/L = 18.2, range = 1.4 to 75.5 [*Sikes et al.*, 1997]). The concentrations are lower than those

reported from the Bering Sea during *E. huxleyi* bloom conditions (ΣC_{37} ng/L mean = 1215, range = 155 to 3120 [*Harada et al.*, 2003]). Alkenones were not detected in 21 of the 50 samples after analysis by GC-FID (detection limit of ~1 ng per compound). Further analysis by GC-CI-MS (detection limit 0.02 ng per compound) measured alkenones in a further five samples, leaving 16 samples
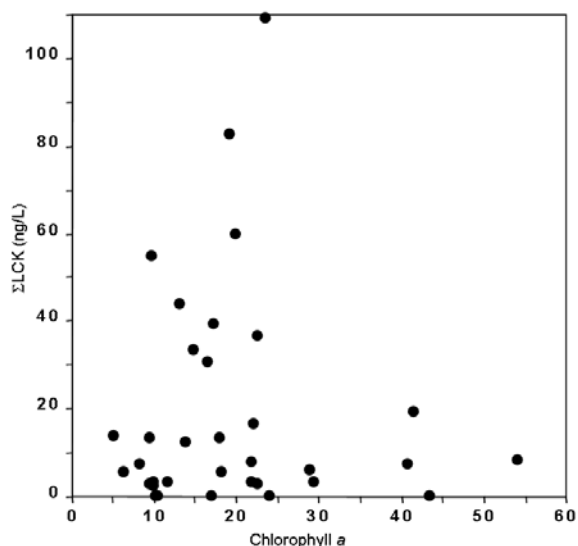
Figure 5. Distributions of ΣLCK (ng/L) versus chlorophyll a (from ship's fluorometer) during cruises JR44 and JR51.

with alkenone contents below our detection limit. Ten of these samples were obtained from the Arctic waters of the Greenland Sea gyre and six from the polar waters of the East Greenland Current (see Figures 1 and 4a). However, alkenones were measured in six of the eleven samples obtained from polar waters in conditions of up to 80% sea ice. The polar waters were distinct from the Arctic and Atlantic water masses by the consistently low alkenone concentrations ($\leq$7.8 ng/L). The highest concentrations (ΣLCK: 30.4–109.5 ng/L) were found in regions influenced by Atlantic source waters, specifically the North Icelandic Irminger Current (NIIC), the Shetland Current (SC) and the Norwegian Atlantic Current (NWAC) (see Figures 1 and 4). However, some low concentrations (<1 ng) were also found in the regions strongly influenced by Atlantic waters.

[21] Fluorescence was measured continuously during both cruises and converted to chlorophyll a concentrations (mg/m^3). It can be considered as a crude measure of phytoplankton standing stock. A plot of alkenone abundance versus chlorophyll a (Figure 5) reveals no significant linear relationship between the concentration of alkenones and the fluorescence measurements, with the highest alkenone concentrations generally measured in samples with chlorophyll a concentrations near the mean (20 mg/m^3). This suggests that nonalkenone producing phytoplankton groups (e.g., diatoms, dinoflagellates, the haptophyte *P. pouchetti*) contributed significantly to the fluorescence signal

and that the productivity of such groups was not tightly correlated with the main producer of the alkenones. This is supported by SeaWiFS data of PIC (a proxy for coccolithophore blooms) which suggest that there were no significant *E. huxleyi* blooms in the Nordic seas during the periods of the two cruises (data not shown) (C. W. Brown, Blooms of the coccolithophorid *Emiliania huxleyi* in global and US coastal waters, 2003, available at http://orbit-net.nesdis.noaa.gov/orad2/doc/ehux.html).

3.3. U^K_{37} and $U^K_{37'}$ in Sea Surface POM During August 1999 and 2000

[22] Scatterplots of $U^K_{37'}$ and U^K_{37} versus SST are illustrated in Figure 6. The measurements of $U^K_{37'}$ on
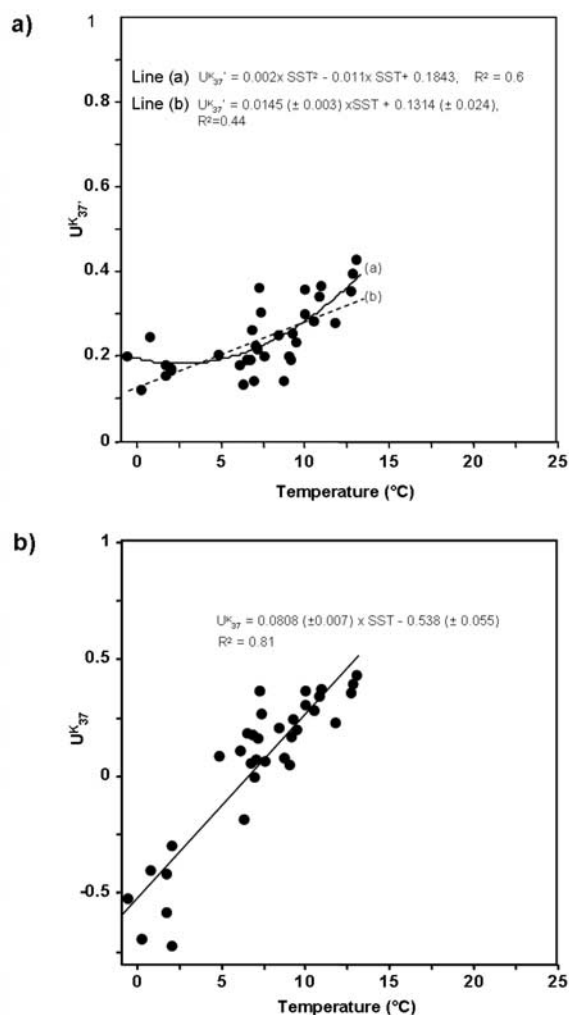

Figure 6. Distributions of (a) $U^K_{37'}$ and (b) U^K_{37} versus SST in POM from the Nordic Seas. Solid lines represent linear regressions; dashed line is a second-order polynomial regression.

Nordic Seas POM had a relatively weak linear correlation with SST:

$$U_{37'}^K = 0.01(\pm0.01) \times SST + 0.13(\pm0.24); R^2 = 0.44, n = 33. \quad (1)$$

This is due, in part, to a loss of correlation between $U_{37'}^K$ and SST below $\sim 8°C$, whereby further decreases in temperature are not accompanied by a fall in the $U_{37'}^K$ index (which does not fall below ~ 0.2). A stronger correlation between $U_{37'}^K$ and SST is achieved with a second-order polynomial regression:

$$U_{37'}^K = 0.002 \times SST^2 - 0.01 \times SST + 0.18; R^2 = 0.6, n = 33. \quad (2)$$

In contrast to $U_{37'}^K$, a much stronger linear correlation exists between U_{37}^K and SST:

$$U_{37}^K = 0.81(\pm0.01) \times SST - 0.54(\pm0.55); R^2 = 0.81, n = 33. \quad (3)$$

This supports the previous suggestion by *Rosell-Melé* [1998] that, on the basis of surficial sediments, U_{37}^K may be preferable to $U_{37'}^K$ as an alkenone SST index in the NE Atlantic and Nordic Seas. The data from this paper show that this observation (a stronger relationship of U_{37}^K to SST than of $U_{37'}^K$ to SST at colder temperatures) is a primary signal occurring in the mixed layer waters as well as in the underlying sediments. Presumably this is due to the linear correlation of the relative abundance of the $C_{37:4}$ compound (which increases in the polar waters) to SST (Bendle et al., submitted manuscript, 2004) and the inclusion of this compound in the U_{37}^K index. Work suggests that water temperature is a strong control on the relative abundance of the $C_{37:4}$ compound under certain culture conditions [*Conte et al.*, 1998] and in a fjordic mesocosm study [*Conte et al.*, 1994]. However, it must be noted that, in open ocean environments the dominant environmental control on the $C_{37:4}$ compound seems more complex (see discussions by Bendle et al. (submitted manuscript, 2004), *Harada et al.* [2003], and *Sicre et al.* [2002]). The cold polar water samples in our data set also display lowered salinities (~ 30 psu), and have significant sea ice cover (which for instance affects light penetration). Such factors may also have influenced alkenones distributions in the East Greenland Current polar waters.

3.4. Comparison of U_{37}^K and $U_{37'}^K$ Distributions With Previously Reported Water Column and Surface Sediment Data

[23] In Figure 7 the new data from this paper are compared with global distributions of $U_{37'}^K$ and U_{37}^K

measured on mixed layer POM. The new data include the first successful measurements of alkenones on water column POM from below 4°C in the North Atlantic; therefore it expands the global water column data set. In Figure 7a the global relationship of water column $U_{37'}^K$ versus SST is illustrated. The culture equation of *Prahl et al* [1988], which is statistically the same as *Muller et al.*'s [1998] core top equation, is included in Figure 7a for reference. A regression of $U_{37'}^K$ versus SST was calculated using a third-order polynomial function; this best represents the reduction in slope of the relationship, at the two ends of the temperature spectrum:

$$U_{37'}^K = -3 \times 10^{-5} \times SST^3 + 1.7 \times 10^{-3} \times SST^2$$
$$+ 7 \times 10^{-3} \times SST + 0.067; \quad (4)$$
$$R^2 = 0.94, n = 245.$$

At SST > 5°C the new Nordic sea data plots within the envelope of previously reported global data [*Conte and Eglinton*, 1993; *Harada et al.*, 2003; *Sicre et al.*, 2002; *Sikes and Sicre*, 2002; *Sikes and Volkman*, 1993; *Ternois et al.*, 1997, 1998]. This reinforces the trend of a systematic difference in slope of the $U_{37'}^K$-temperature relationship, between that derived from water column POM and that derived from culture by *Prahl et al.* [1988] and from core tops by *Muller et al.* [1998]. Thus, for a given water temperature and particularly between $\sim 5-15°C$, sediments yield a higher $U_{37'}^K$ value than in the water column POM, confirming a trend previously recognized [e.g., *Conte et al.*, 2001; *Rosell-Melé et al.*, 1995c].

[24] The form of the global water column regression compares with results from culture experiments with a number of *E. huxleyi* and *G. oceanica* strains from different ocean basins [*Conte et al.*, 1998]. The *Conte et al.* [1998] study reported a reduction of slope in the calibration of $U_{37'}^K$ to temperatures <12°C and >21°C (for some strains) and suggested that due to such interstrain differences, locally derived SST calibrations may be preferable to applying the *Prahl et al.* [1998] equation globally. However, such work does not explain the offset between global surficial sediments (which mostly follow the form of the *Prahl et al.* [1998] equation and water column POM data. This has raised questions about what factors control the export of alkenone material, produced in the euphotic zone, to depth and how these may influence the alkenone signature imparted to sediments [*Herbert*, 2001, and references therein]. The discrepancy is poorly understood, but aspects of
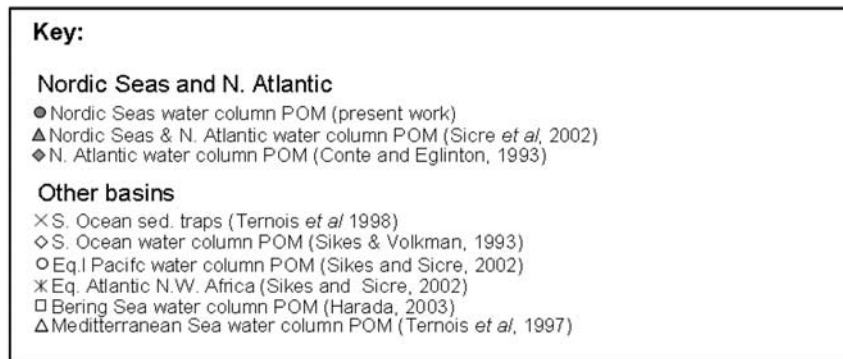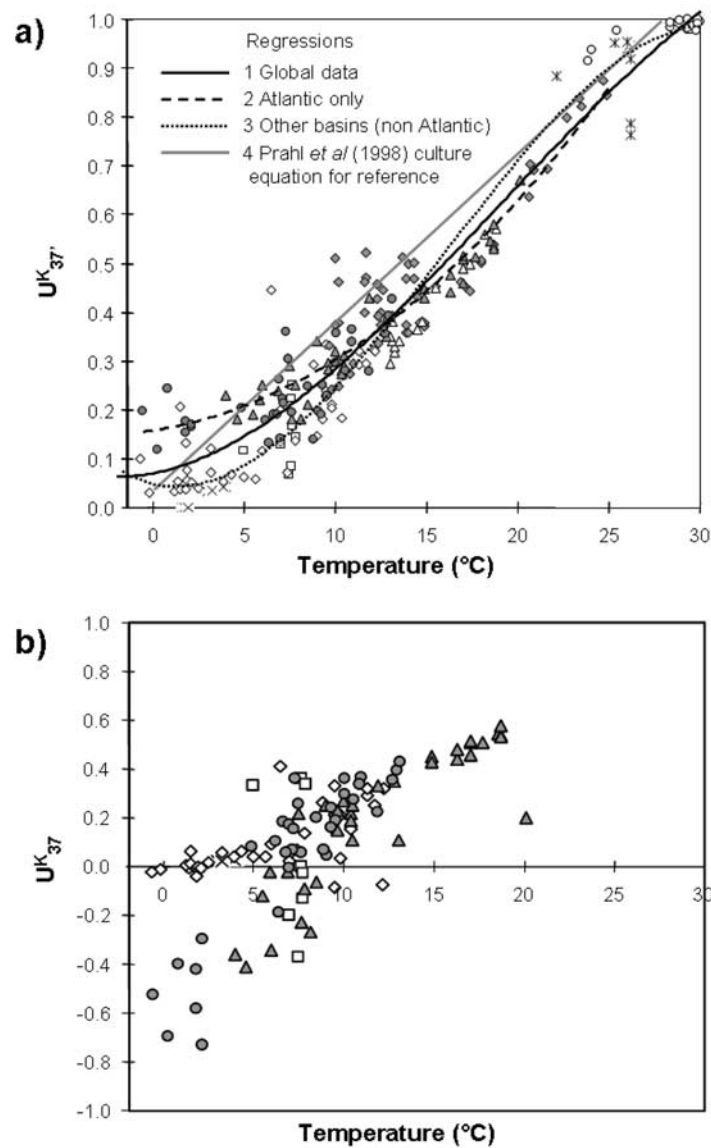
Figure 7.   Distributions of (a) $U_{37'}^{K}$ and (b) U_{37}^{K} measured on mixed layer POM versus water temperature. Data are from this thesis and reported in literature. Regressions 1 and 3 are third-order polynomial and regression 2 is second-order polynomial, as described in the text.

the genetics, physiology and the seasonal ecology/ flux of alkenone-producing haptophytes may be responsible [*Bijma et al.*, 2001, and references therein].

[25] At temperatures below 5°C, there is a distinct separation in the field of $U^K_{37'}$-temperature data between the new observations from the Nordic Seas data and those from the Southern Ocean. So that for a given growth temperature the $U^K_{37'}$ value in the Nordic Seas is ~0.1 units higher than the $U^K_{37'}$ value for the Southern Ocean. This deviation is emphasized by regressions (illustrated in Figure 7a) derived using North Atlantic and non-Atlantic data only. A similar divergence in temperature dependence of the $U^K_{37'}$ index relationship has also been noted for surficial sediments of the northern North Atlantic and the Southern Ocean [*Rosell-Melé*, 1998]. The new Nordic Seas water column data suggest that a significant part of the trend observed in the surficial sediments has a genuine biological component.

[26] If the expanded global water column database is used to plot U^K_{37} versus SST then the divergence of values for the Nordic Seas and Southern ocean (compared to $U^K_{37'}$) is accentuated (Figure 7b). This is due to the much higher concentrations of $C_{37:4}$ observed in northern waters [*Conte et al.*, 1994; *Sicre et al.*, 2002; Bendle et al., submitted manuscript, 2004]. In the surficial sediments of the Nordic Seas there is no significant correlation between $U^K_{37'}$ and SST below ~10°C [*Rosell-Melé*, 1998]. This lack of a correlation is also observed in the regression of $U^K_{37'}$ measured on the new Nordic Seas water column POM data <8°C:

$$U^K_{37'} = 0.008(\pm0.004) \times SST + 0.16(\pm0.02);$$

$$R^2 = 0.14, n = 19.$$

(5)

However, the relationship of U^K_{37} to SST measured on Nordic Seas water column POM <8°C is stronger:

$$U^K_{37} = 0.082(\pm0.012) \times SST - 0.63(\pm0.07);$$

$$R^2 = 0.81, n = 19.$$

(6)

On the basis of surficial sediments it has been suggested that the U^K_{37} index is used to calculate SSTs in the Nordic Seas region, rather than $U^K_{37'}$ [*Rosell-Melé*, 1998]. The data from this study suggest that U^K_{37} does indeed have a stronger relationship to SST than $U^K_{37'}$ at cold temperatures (<8°C) in the Nordic Seas. However, it is worth noting that due to the high abundances of the $C_{37:4}$ compound in these samples negative values of the U^K_{37} index are derived for the colder temperature samples. The work which first proposed the U^K_{37} equation [*Brassell et al.*, 1986b] never justified the subtraction of the $C_{37:4}$ compound from $C_{37:2}$ in the numerator. The work in the largely unpublished thesis by *Marlowe* [1984] suggests that the formula of U^K_{37} was derived by an empirical trial an error process until obtaining an index that afforded the best linear fit with growth temperature from cultured algae. Whereas the $U^K_{37'}$ index is conceptually straightforward, there is no apparent biochemical rationale for the form of the numerator in U^K_{37}. An alternative index to estimate SST for samples where $C_{37:4}$ values are significantly high could take the form of

$$U^K_{37}* = \frac{C_{37:2}}{C_{37:2} + C_{37:3} + C_{37:4}}.$$

Indeed, when this equation is used and the data are plotted against SST (Figure 8c), the result is similar to $U^K_{37'}$ at SSTs >6°C (Figure 8a), but unlike $U^K_{37'}$ below 6°C, values of $U^K_{37}*$ still decline with SST. This suggests that $U^K_{37}*$ could be a preferable index to apply in high latitude environments. However, as illustrated by Figure 8 whatever index is used there are major discrepancies in the distributions of water column POM and surficial sediments values in the Nordic Seas. Therefore any SST calibration based on water column data may have little practical application to SST reconstruction in sediment cores in parts of the region. This contrasts with the Southern Ocean, where the equation for sedimentary $U^K_{37'}$ and summer SSTs agrees with that from surface water POM [*Sikes et al.*, 1997].

3.5. Reassessing the Limits of Alkenone Indices

[27] The data described above highlight a challenge in the application of alkenone indices for paleotemperature work in the Nordic Seas. For a given SST, there is a shift toward higher values in the alkenone indices in sediments in comparison to those in POM, and the difference between sedimentary and POM values increases with decreasing SSTs. This is further complicated by considerable scatter in the calibration of the sediment data (Figure 8). A greater understanding of the processes intervening between alkenone synthesis in the water column, deposition and burial in the sediments is necessary if alkenones are to be applied with confidence in the Nordic Seas. Two obvious
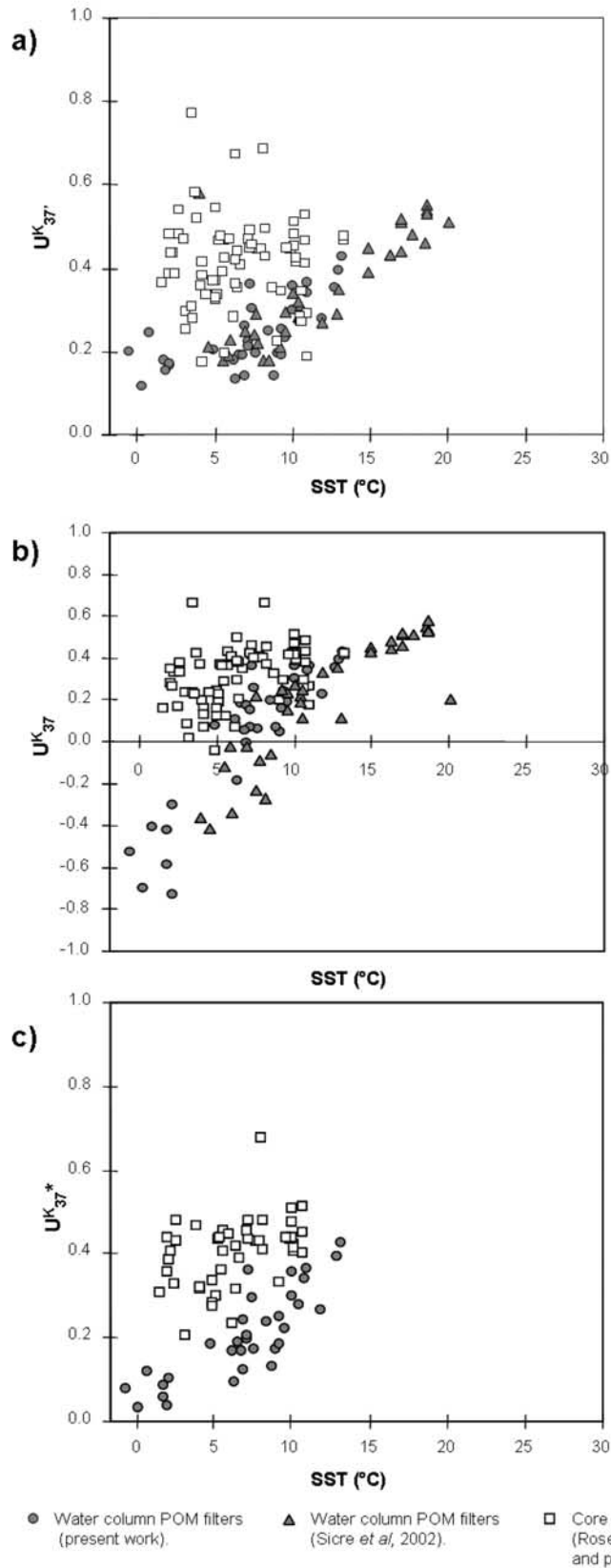
Figure 8. Nordic Seas distributions of (a) U$^{K}_{37'}$, (b) U$^{K}_{37}$, and (c) U$^{K}_{37}$* measured on mixed layer POM and surface sediments versus water temperature. Data are from this thesis and reported in literature.

processes may be responsible for the observed discrepancies. One could be the diagenetic alternation of the autochthonous alkenone signal in the water column and during subsequent burial in the sediments. Thus diagenesis has been proposed as a mechanism to bias the sedimentary signal, whereby the more unsaturated components could be preferentially removed or degraded [e.g., *Hoefs et al.*, 1998]. Nevertheless, so far no conclusive data have been provided to support a preferential diagenetic alteration of one alkenone over the other, either for the $C_{37:3}$ compound (see review by *Grimalt et al.* [2000]) or the $C_{7:4}$ compound [*Flügge*, 1997; Bendle et al., submitted manuscript, 2004].

[28] The other process could be caused by advection of sediments and the occurrence of mixtures of autochthonous and allochthonous components in surficial sediments. Recent compound specific radiocarbon work has highlighted that in certain oceanic environments (Benguela upwelling system, Bermuda rise) alkenone records in sediments may include a significant allochthonous (older) component [*Mollenhauer et al.*, 2003; *Ohkouchi et al.*, 2002]. For the Nordic Seas *Thomsen et al.* [1998] suggested that resuspension and lateral advection of alkenone bearing material was common place. Turbulent plume events originating on the Barents sea continental margin could transport significant quantities of allochthonous alkenones and TOC to the Norwegian Sea [*Martrat et al.*, 2003; *Thomsen et al.*, 1998]. Winnowing of fine sediments by bottom currents has also been observed as a significant process on continental shelves around the Norwegian-Greenland Sea [*Cadman*, 1996; *Vorren et al.*, 1984]. However, *Flügge* [1997] found that alkenone indices were not significantly biased in deep sediment traps (compared with mixed layer traps) in the Lofoten basin (Norwegian Sea).

[29] Indirect evidence of potential alkenone bias in the Nordic Seas also comes from sediment traps which record coccolithophore assemblages. These show that temporal and regional input of resuspended material to depth is highly variable [*Andruleit*, 1997; *Samtleben et al.*, 1995]. Overall the evidence suggests that a warm bias may "overprint" the local signal by advection and that this is more severe in the Greenland Sea than in the Norwegian Sea. For example, sediments of the southeast Greenland margin can contain coccoliths from species of subtropical and midlatitudinal areas (B. Balestra et al., Coccolithophorids in the Southeast Greenland Margin: Production and sedimentation, submitted to *Marine Micropaleontology*, 2004).

[30] Therefore sediment advection is an important process in the Nordic Seas region and hence is a probable source of error for alkenone indices (and possibly other proxies). Does this mean that entire region should be considered as too problematic for alkenone based paleoceanographic research? If the biasing influence of allochthonous material is limited geographically within the Nordic Seas then certain areas may still be viable for paleoceanographic studies. In Figure 9 the geographic distribution of the core top $U^K_{37'}$ values that are responsible for the larger deviations in the $U^K_{37'}$-SST regression are highlighted. The "anomalous" samples are defined as those that lie outside the *Muller et al.* [1998] core top equation data envelope. We can only attempt this comparison for $U^K_{37'}$ as no equivalent global core top database exists for U^K_{37}. The figure shows that the "anomalous" samples are confined to the core tops from the East Greenland Shelf, the Greenland Basin, Mohns ridge, northern Iceland Plateau, upper Bear Island Fan and North Sea Fan. This may be expected for the Greenland Shelf, Greenland Basin and north Icelandic Plateau as these areas are dominated by cold Polar and Arctic water masses and in Figure 6a we demonstrated that the $U^K_{37'}$-SST relationship was not maintained in the Nordic Seas surface waters (summer of 1999 and 2000) below ~8°C. However, "anomalous" samples from the Bear Island and North Sea Fans are from regions dominated by Atlantic signature surface waters. In these cases we suggest that these samples have been biased by a component of reworked or allochthonous alkenones perhaps originating from the continental shelf [*Martrat et al.*, 2003; *Thomsen et al.*, 1998]. Measurements of potentially misleading proxy values from certain Nordic seas localities are even more likely for periods such as the last glacial maximum, when glacial processes contributed to the reworking of sediments by debris flows at the major through mouth fans along the East Greenland and Norwegian margins (i.e., North Sea, Scorsby Sund and Bear Island Fans) [*Ó Cofaigh et al.*, 2004]. It is therefore the key to define localities where such processes of lateral advection may not be occurring. For instance the surface samples from the northern Atlantic, Icelandic Shelf, Norwegian and Lofoten Basins yield $U^K_{37'}$ values that fall within the *Muller et al.* [1998] data envelope. This suggests that accurate alkenone SST estimates in the Nordic seas are geographically constrained, but that data from the latter sites may yield reliable paleoceanographic reconstructions of SST at least during the Holocene or when ocean-
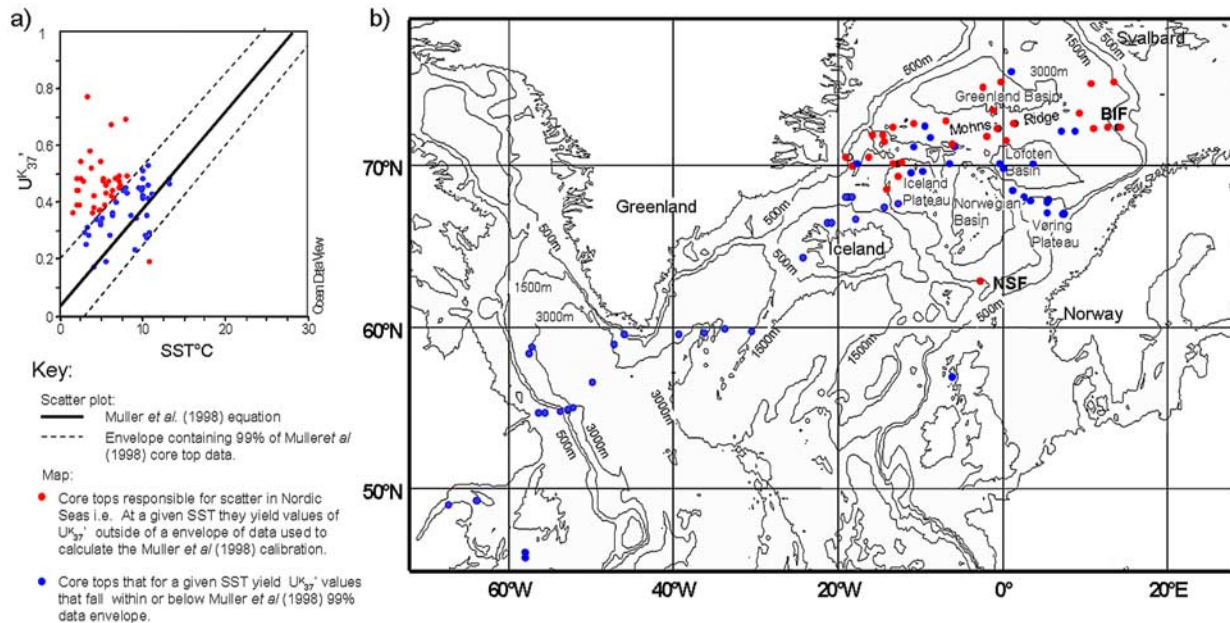
Figure 9. (a) Identification and (b) geographic distribution of core top Nordic Seas samples that create scatter in the $U^K_{37'}$ index relative to *Muller et al.*'s [1998] core top calibration.

ographical and depositional conditions were similar to the present.

4. Conclusions

[31] Alkenones were measured in filtered particulate organic matter (POM) from the summer surface waters (1999 and 2000) of the Nordic Seas (including a number of samples collected from polar waters in conditions of up to 80% sea ice). Values of $U^K_{37'}$ from the new Nordic Seas POM data show no correlation with SST below 8°C. In contrast to $U^K_{37'}$, a stronger linear correlation exists between U^K_{37} and SST ($R^2 = 0.69$) for the temperature range 0–12°C. This supports previous suggestions, based on surficial sediment data, that overall, U^K_{37} may be a more appropriate index for the Nordic Seas than $U^K_{37'}$ [*Rosell-Melé et al.*, 1995c]. However, dominant control of the abundance of the tetraunsaturated alkenone still remains to be clarified and thus this may constrain U^K_{37} as a proxy to estimate SST in low temperature locations. This also reinforces the need for future studies to report $C_{37:4}$ concentrations (along with $C_{37:2}$ and $C_{37:3}$).

[32] Comparison of the new sea surface POM $U^K_{37'}$ data with a global database reinforces the trend of a systematic difference in the slope of the $U^K_{37'}$ versus SST relationship between that derived from water column POM and that derived from culture by *Prahl et al.* [1988] and from core tops by *Muller et*

al. [1998]. Whereby, the POM data generally lie in a field that gives warmer-than-predicted growth temperatures at a given $U^K_{37'}$, particularly between ~5–15°C. At temperatures below 5°C there is a distinct separation in the field of $U^K_{37'}$ versus temperature data, between the new observations from the Nordic Seas and observations from the Southern Ocean.

[33] The new $U^K_{37'}$ and U^K_{37} data highlight major differences between the spatial distributions of U^K_{37} and $U^K_{37'}$ in the water column POM and surficial sediments of the Nordic Seas for both indices. An examination of the geographic locations that are responsible for the scatter in the $U^K_{37'}$ versus SST relationship in surficial sediments of the Nordic Seas shows a clear geographical division suggesting that East Greenland Shelf, the Greenland Basin, Mohns ridge, northern Iceland Plateau and upper Bear Island Fan are associated with the anomalous values. We suggest that the breakdown of the sedimentary $U^K_{37'}$-SST relationship in these regions is due to both biological limitations (e.g., Greenland Shelf and Basin) or inclusion of an autochthonous alkenone component (e.g., Bear Island Fan and North Sea Fan). Samples from the northern Atlantic, Icelandic Shelf, Norwegian basin, and Lofoten Basin yielded $U^K_{37'}$ values that fall within the expected range, based on the global core top calibration [*Muller et al.*, 1998]. We suggest that accurate alkenone derived SST estimates in the Nordic seas

are geographically delimited but that data from localities such as the latter sites, at least, may yield reliable paleoceanographic reconstructions of SST when oceanographical and depositional conditions were similar to the present.

Acknowledgments

References

Andruleit, H. A. (1997), Coccolithophore fluxes in the Norwegian-Greenland Sea: Seasonality and assemblage alterations, *Mar. Micropaleontol.*, *31*, 45–64.

Bacon, S., and M. J. Yelland (1999), RRS *James Clark Ross* Cruise 44, *Cruise Rep. 33*, 140 pp., Southampton Oceanogr. Cent., Southampton, UK.

Bendle, J. A. (2003), Palaeoceanography of the Holocene and Late-Glacial N.E. Atlantic: Development and application of biomarker proxies of environmental change, Ph.D. thesis, Univ. of Durham, Durham, UK.

Bijma, J., M. Altabet, M. Conte, H. Kinkel, G. J. M. Versteegh, J. K. Volkman, S. G. Wakeham, and P. P. Weaver (2001), Primary signal: Ecological and environmental factors—Report from Working Group 2, *Geochem. Geophys. Geosyst.*, *2*, doi:10.1029/2000GC000051.

Brassell, S. C. (1993), Application of biomarkers for delineating marine paleoclimatic fluctuations during the pleistocene, in *Organic Geochemistry: Principles and Applications*, edited by M. H. Engel and S. A. Macko, pp. 699–738, Plenum, New York.

Brassell, S. C., R. G. Brereton, G. Eglinton, J. Grimalt, G. Liebezeit, I. T. Marlowe, U. Pflaumann, and M. Sarnthein (1986a), Palaeoclimatic signals recognized by chemometric treatment of molecular stratigraphic data, *Org. Geochem.*, *10*, 649–660.

Brassell, S. C., G. Eglinton, I. T. Marlowe, U. Pflaumann, and M. Sarnthein (1986b), Molecular stratigraphy: A new tool for climatic assessment, *Nature*, *320*, 129–133.

Broecker, W. S., and G. H. Denton (1989), The role of ocean-atmosphere reorganization in glacial cycles, *Geochim. Cosmochim. Acta*, *53*(10), 2465–2501.

Cadman, V. M. (1996), Clacimarine sedimentation and environments during the Late Weishselian and Holocene in the Bellsund Trough and Van Keulenfjordent, Svalbard, Ph.D. thesis, Univ. of Cambridge, Cambridge, UK.

Conkright, M. E., et al. (1998), *World Ocean Database* [CD-ROM], Natl. Oceanic and Atmos. Admin., U.S. Dep. of Commer., Silver Spring, Md.

Conte, M. H., and G. Eglinton (1993), Alkenone and alkenoate distributions within the euphotic zone of the eastern North Atlantic: Correlation and production temperature, *Deep Sea Res., Part I*, *40*, 1935–1961.

Conte, M. H., G. Eglinton, and L. A. S. Madureira (1992), Long-chain alkenones and alkyl alkenoates as palaeotemperature indicators: Their production, flux and early sedimentary diagenesis in the Eastern North Atlantic, *Org. Geochem.*, *19*, 287–298.

Conte, M. H., A. Thompson, and G. Eglinton (1994), Primary production of lipid biomarker compounds by *Emiliania huxleyi*. Results from an experimental mesocosm study in fjords of southwestern Norway, *Sarsia*, *79*, 319–331.

Conte, M. H., A. Thompson, D. Lesley, and P. G. Harris (1998), Genetic and physiological influences on the alkenone/alkenoate versus growth temperature relationship in *Emiliania huxleyi* and *Gephyrocapsa oceania*, *Geochim. Cosmochim. Acta*, *62*(1), 51–68.

Conte, M. H., J. C. Weber, L. L. King, and S. G. Wakeham (2001), The alkenone temperature signal in western North Atlantic surface waters, *Geochim. Cosmochim. Acta*, *65*(23), 4275–4287.

Dickey, T., J. Marra, M. Stramska, C. Langdon, T. Granata, A. Plueddemann, R. Weller, and J. Yoder (1994), Bio-optical and physical variability in the subarctic North Atlantic Ocean during the spring of 1989, *J. Geophys. Res.*, *99*(C11), 22,541–22,556.

Dickson, R. R., and J. Brown (1994), The production of North Atlantic Deep Water, sources, rates, and pathways, *J. Geophys. Res.*, *99*, 12,319–12,341.

Flügge, A. (1997), Jahreszeitliche Variabilität von ungesättigten C37 Methylketonen (Alkenone) in Sinkstoffallenmaterial der Norwegischen See und deren Abbildung in Oberflächensedimenten, Ph.D., Univ. of Keil, Keil, Germany.

Freeman, K. H., and S. G. Wakeham (1991), Variations in the distributions and isotopic compositions of alkenones in Black Sea particles and sediments, *Adv. Org. Geochem.*, *19*(1–3), 277–285.

Grimalt, J. O., J. Rullkötter, M. Sicre, R. Summons, J. Farrington, H. R. Harvey, M. Goñi, and K. Sawada (2000), Modifications of the C_{37} alkenone and alkenoate composition in the water column and sediment: Possible implications for sea surface temperature estimates in paleoceanography, *Geochem. Geophys. Geosyst.*, *1*, doi:10.1029/2000GC000053.

Hansen, B., and S. Østerhus (2000), North Atlantic-Nordic Seas exchanges, *Progr. Oceanogr.*, *45*, 109–208.

Harada, N., K. H. Shin, A. Murata, M. Uchida, and T. Nakatani (2003), Characteristics of alkenones synthesized by a bloom of *Emiliania huxleyi* the Bering Sea, *Geochim. Cosmochim. Acta*, *67*(8), 1507–1519.

Herbert, T. D. (2001), Review of alkenone calibrations (culture, water column, and sediments), *Geochem. Geophys. Geosyst.*, *2*, doi:10.1029/2000GC000055.

Hoefs, M. J. L., G. J. M. Versteegh, W. I. C. Rijpstra, J. W. de Leeuw, and J. S. S. Damste (1998), Postdepositional oxic degradation of alkenones: Implications for the measurement of palaeo sea surface temperatures, *Paleoceanography*, *13*(1), 42–49.

Johanessen, O. M. (1986), Brief overview of the physical oceanography, in *The Nordic Seas*, edited by B. G. Hurdle, pp. 103–127, Springer-Verlag, New York.

Kornilova, O., and A. Rosell-Melé (2003), Application of microwave-assisted extraction to the analysis of biomarker climate proxies in marine sediments, *Org. Geochem.*, *34*(11), 1517–1523.

Lalli, C. M., and T. R. Parsons (1997), *Biological Oceanography: An Introduction*, Butterworth-Heinemann, Woburn, Mass.

Levitus, S., and T. Boyer (1994), *World Ocean Atlas 1994*, vol. 4, *Temperature*, Natl. Oceanic and Atmos. Admin., U.S. Dep. of Commer., Silver Spring, Md.

Longhurst, A. L. (1998), *Ecological Geography of the Sea*, Academic, San Diego, Calif.

Madureira, L. A. S., M. H. Conte, and G. Eglinton (1995), Early diagenesis of lipid biomarker compounds in North Atlantic sediments, *Paleoceanography*, *10*, 627–642.

Marlowe, I. (1984), Lipids as palaeoclimatic indicators, thesis, Univ. of Bristol, Bristol, UK.

Martrat, B., J. O. Grimalt, J. Villanueva, S. van Kreveld, and M. Sarnthein (2003), Climatic dependence of the organic matter contributions in the north eastern Norwegian Sea over the last 15,000 years, *Org. Geochem.*, *34*(8), 1057–1070.

Mollenhauer, G., T. I. Eglinton, N. Ohkouchi, R. R. Schneider, P. J. Muller, P. M. Grootes, and J. Rullkotter (2003), Asynchronous alkenone and foraminifera records from the Benguela upwelling system, *Geochim. Cosmochim. Acta*, *67*(12), 2157–2171.

Muller, P. J., G. Kirst, G. Ruhland, I. von Storch, and A. Rosell-Melé (1998), Calibration of the alkenone paleotemperature index $U^K_{37'}$ based on core-tops from the eastern South Atlantic and the global ocean (60 degrees N–60 degrees S), *Geochim. Cosmochim. Acta*, *62*(10), 1757–1772.

Ó Cofaigh, C., J. Taylor, J. A. Dowdeswell, A. Rosell-Melé, N. H. Kenyon, J. Mienert, and J. Evans (2004), Geological evidence for sediment reworking in the Norwegian-Greenland Sea and its palaeoceanograhic implications, *Geol. Soc. Spec. Publ.*, in press.

Ohkouchi, N., T. I. Eglinton, L. D. Keigwin, and J. M. Hayes (2002), Spatial and temporal offsets between proxy records in a sediment drift, *Science*, *298*, 1224–1227.

Pelejero, C., and E. Calvo (2003), The upper end of the $U^K_{37'}$ temperature calibration revisited, *Geochem. Geophys. Geosyst.*, *4*, 1014, doi:10.1029/2002GC000431.

Prahl, F. G., and L. A. Muehlhausen (1989), An organic geochemical assessment of oceanographic conditions at Manop site C over the past 26,000 years, *Paleoceanography*, *4*, 495–510.

Prahl, F. G., and S. G. Wakeham (1987), Calibration of unsaturation patterns in long-chain ketone compositions for paleotemperature assessment, *Nature*, *330*(6146), 367–369.

Prahl, F. G., L. A. Muehlhausen, and D. L. Zahnle (1988), Further evaluation of long-chain alkenones as indicators of paleoceanographic conditions, *Geochim. Cosmochim. Acta*, *52*(9), 2303–2310.

Prahl, F., T. Herbert, S. C. Brassell, N. Ohkouchi, M. Pagani, D. Repeta, A. Rosell-Melé, and E. Sikes (2000), Status of alkenone paleothermometer calibration: Report from Working Group 3, *Geochem. Geophys. Geosyst.*, *1*, doi:10.1029/2000GC000058.

Rosell-Melé, A. (1998), Interhemispheric appraisal of the value of alkenone indices as temperature and salinity proxies in high-latitude locations, *Paleoceanography*, *13*(6), 694–703.

Rosell-Melé, A., J. Carter, and G. Eglinton (1993), Distribution of long-chain alkenones and alkyl alkenoates in marine surface sediments from the North East Atlantic, *Org. Geochem.*, *22*, 501–509.

Rosell-Melé, A., J. Carter, A. Parry, and G. Eglinton (1995a), Determination of the UK37 index in geological samples, *Anal. Chem.*, *67*(7), 1283–1289.

Rosell-Melé, A., J. Carter, A. Parry, and G. Eglinton (1995b), Novel procedure for the determination of the UK37 index in sediment samples, *Anal. Chem.*, *67*, 1283–1289.

Rosell-Melé, A., G. Eglinton, U. Pflaumann, and M. Sarnthein (1995c), Atlantic core-top calibration of the UK37 index as a sea-surface palaeotemperature indicator, *Geochim. Cosmochim. Acta*, *59*(15), 3099–3107.

Samtleben, C., P. Schäfer, H. Andruleit, A. Baumann, K.-H. Baumann, A. Kohly, J. Matthiessen, and A. Schröder-Ritzrau (1995), Plankton in the Norwegian-Greenland Sea: From living communities to sediment assemblages—An actualistic approach, *Geol. Rundsch.*, *84*, 108–136.

Schulz, H. M., A. Schoner, and K. C. Emeis (2000), Long-chain alkenone patterns in the Baltic Sea—An ocean-freshwater transition, *Geochim. Cosmochim. Acta*, *64*(3), 469–477.

Sicre, M., E. Bard, U. Ezat, and F. Rostek (2002), Alkenone distributions in the North Atlantic and Nordic sea surface waters, *Geochem. Geophys. Geosyst.*, *3*, 1013, doi:10.1029/2001GC000159.

Sikes, E. L., and M. Sicre (2002), Relationship of the tetra-unsaturated C_{37} alkenone to salinity and temperature: Implications for paleoproxy applications, *Geochem. Geophys. Geosyst.*, *3*, 1063, doi:10.1029/2002GC000345.

Sikes, E. L., and J. K. Volkman (1993), Calibration of alkenone unsaturation ratios (uk37) for paleotemperature estimation in cold polar waters, *Geochim. Cosmochim. Acta*, *57*, 1883–1889.

Sikes, E. L., J. K. Volkman, L. G. Robertson, and J. J. Pichon (1997), Alkenones and alkenes in surface waters and sediments of the Southern Ocean: Implications for paleotemperature estimation in polar regions, *Geochim. Cosmochim. Acta*, *61*(7), 1495–1505.

Sonzogni, C., E. Bard, F. Rostek, A. Lafont, A. Rosell-Melé, and G. Eglinton (1997), Core-top calibration of the alkenone index versus sea surface temperature in the Indian Ocean, *Deep Sea Res., Part II*, *44*, 1445–1460.

Swift, J. H. (1986), The Arctic waters, in *The Nordic Seas*, edited by B. G. Hurdle, pp. 129–153, Springer-Verlag, New York.

Teece, M. A., J. M. Getlife, J. W. Leftley, R. J. Parkes, and J. R. Maxwell (1998), Microbial degradation of the marine prymnesiophyte Emiliania huxleyi under oxic and anoxic conditions as a model for early diagenesis: Long chain alkadienes, alkenones and alkyl alkenoates, *Org. Geochem.*, *29*, 863–880.

Ternois, Y., M. A. Sicre, A. Boireau, M. H. Conte, and G. Eglinton (1997), Evaluation of long-chain alkenones as paleo-temperature indicators in the Mediterranean Sea, *Deep Sea Res., Part I*, *44*, 271–286.

Ternois, Y., M. A. Sicre, A. Boireau, L. Beaufort, J. C. Miquel, and C. Jeandel (1998), Hydrocarbons, sterols and alkenones in sinking particles in the Indian Ocean sector of the Southern Ocean, *Org. Geochem.*, *28*, 489–501.

Thomsen, C., D. E. Schulz-Bull, G. Petrick, and J. C. Duinker (1998), Seasonal variability of the long-chain alkenone flux and the effect on the U37k'-index in the Norwegian Sea, *Org. Geochem.*, *28*(5), 311–323.

Vorren, T. O., M. Hald, and E. Thomsen (1984), Quaternary sediments and environments on the continental shelf off northern Norway, *Mar. Geol.*, *57*, 229–257.